

# Machine learning-based Prediction for Drug-Drug Interaction Using a Knowledge Graph

Golnaz Taheri<sup>1,#</sup>, Mahnaz Habibi<sup>2,#</sup>, and Tahereh Sedghamiz<sup>3</sup>

<sup>1</sup> Department of Computer and Systems Sciences, Stockholm University, Stockholm, Sweden.

{golnaz.taheri}@dsv.su.se

<sup>2</sup> Department of Mathematics, Qazvin Branch, Islamic Azad University, Qazvin, Iran.

<sup>3</sup> Department of Drug Science and Technology, University of Turin, Italy.

# These authors contributed equally.

**Abstract.** The treatment of complex diseases often involves the use of multiple drugs, a practice known as polypharmacy. However, this approach comes with the risk of drug-drug interactions (DDIs), which can lead to unanticipated adverse effects and even toxicity. Therefore, ensuring the safety of polypharmacy requires identifying DDIs and exploring their underlying mechanisms. Traditional wet lab methods for detecting DDIs are expensive and time-consuming, while computational methods have been developed to predict DDIs. Many of these methods have limitations, and they often struggle to predict potential DDIs between known drugs in the DDI network and drugs from outside that network without any connections to other drugs. Moreover, they may lack the capability to delve into the underlying mechanisms of DDIs and provide meaningful interpretations. In response to these challenges, we introduce a novel machine learning-based method called NGMG, which leverages a knowledge graph to identify feature representations for each drug based on its chemical and topological properties in the DDI network. Then, it combines these features for each drug pair and feeds them into a predictor to obtain a final DDI prediction score. Our experimental results demonstrate the effectiveness of NGMG in two crucial DDI prediction scenarios: identifying potential DDIs among known drugs within the DDI network and predicting interactions between drugs within the DDI network and some drugs from outside the network without any connections to other drugs.

**Keywords:** Drug Drug Interaction · feature representation · Machine Learning · knowledge graph.

## 1 Introduction

In recent years, polypharmacy, also referred to as combination drug therapy, has emerged as a promising strategy for treating complex diseases such as cancer and diabetes [1]. This approach involves combining different medications

to enhance therapeutic outcomes. For example, in the treatment of metastatic hepatocellular carcinoma, Pembrolizumab has been effectively combined with Sorafenib, and in the management of Parkinson’s disease, Entacapone has been used to increase the plasma concentration of Levodopa, resulting in improved therapeutic effects [2, 3]. However, it’s essential to recognize that concurrently using two or more drugs can lead to Drug-Drug interactions (DDIs), which may induce pharmacological changes with potential consequences, including side effects, adverse reactions, and severe toxicity [4]. As the demand for polypharmacy treatments continues to grow, there is an urgent need to identify DDIs. Nevertheless, the traditional methods of detecting these interactions on a large scale, both in vitro and in vivo, can be expensive and time-consuming. To address this challenge, computational approaches have been developed, particularly machine learning-based methods, to predict and screen potential drug-drug interactions efficiently.

As cost-effective and efficient, various machine learning techniques have demonstrated their potential in offering an initial screening of DDIs for subsequent experimental confirmation [5, 6]. Typically, these models are trained using established DDIs to predict potential interactions among many unlabeled drug pairs. Training incorporates a variety of drug-related characteristics, encompassing factors like chemical structure [7–9], targets [7, 10, 11], anatomical taxonomy [11, 12], and phenotypic observations [10, 11]. These models reframe the task of predicting DDIs from a simple ‘yes or no’ interaction into a binary classification challenge. These methods are commonly executed using established classifiers such as SVM [8], logistic regression [12], decision trees, and naive Bayes [13]. Alternatively, they may utilize network propagation to reason through drug-drug network structures [14], employ label propagation [15], apply random walk techniques [7] or matrix factorization methods [9, 10]. Graph network methods [17] also offer promising avenues in drug development and discovery. These methods are particularly valuable for tasks like molecular activity prediction, drug side effect prediction [9], drug target interactions prediction [17], and drug response [19–21]. These methods play a crucial role in drug-drug interaction prediction, which enhances traditional binary DDI prediction. For instance, in the case of NDD [22], they computed a drug similarity matrix from multiple drug properties and utilized a multilayer deep learning classifier to predict binary DDIs. Similarly, Wang et al. [23] employed GCN to extract drug representation features from DDI networks, which were then fed into a three-layer multilayer perception for binary DDI prediction. While these approaches delivered promising results, they exhibited certain limitations. First, these methods relying on the DDI network’s topological information for feature extraction may overlook new drugs with no existing links in the DDI network. Second, current deep-learning techniques cannot interpret drug interactions, making it challenging to understand the underlying mechanisms of these interactions. Third, these models primarily emphasize the connections between nodes while overlooking node attributes and edge types [24]. To address the knowledge gaps created by graph embedding

algorithms, there is a growing emphasis on knowledge graph-based methods [25] at present.

We introduce a novel approach, NGMG, to predict DDIs. NGMG constructs a knowledge graph representation for each drug based on its chemical and topological features. We then focus on the learned features for each drug pair, using them as predictors to derive DDI prediction scores for pairs of drugs, even when they are not directly linked to other drugs. NGMG employs multi-step operations to capture different substructure groups of drugs within the constructed graph, generating effective feature representations. Our experimental results demonstrate that NGMG excels at predicting potential DDIs among drugs within the DDI network, as well as new drugs outside the network. NGMG enhances interpretability and uncovers the underlying mechanisms of interactions between drug pairs.

## 2 Materials and methods

### 2.1 Datasets

We first built the DDI dataset that contains 4,349 drugs and 179,347 drug-drug interactions from DrugBank 5.0 [22]. We downloaded the completed XML formatted database (including the comprehensive profiles of 16,558 drugs) and parsed all approved small-molecule drugs and their DDI entries. We extracted the drugs’ chemical structure information using Simplified Molecular Input Line Entry System (SMILES) strings from the XML file provided by DrugBank and extracted chemical features from their SMILES. These drug molecules were taken as the input nodes for the knowledge graph to obtain the drug feature vectors. In this graph, the edges represent the connection between drugs. NGMG learns the drug representation features directly from their chemical molecular and topological structures.

### 2.2 Problem Formulation

Consider the graph  $G$ , denoted as  $G = \langle V, E \rangle$ , which represents the DDI network. In this context, the set  $V$  corresponds to the drugs involved, while the set  $E$  indicates the interactions between these drugs. The network size is represented by  $|V| = n$ , indicating the number of nodes, and  $|E| = m$ , indicating the number of edges. If an edge  $uv$  is present in the set  $E$ , nodes  $u$  and  $v$  are referred to as neighbors. The set  $N(u)$  represents all the neighbors of a given node  $u$ . The Jaccard similarity between two vertices,  $u$  and  $v$ , is defined as follows:

$$J_{sim}(u, v) = \frac{|N(u) \cap N(v)|}{|N(u) \cup N(v)|} \quad (1)$$

**Chemical matching coefficient:** Let  $\mathcal{G} = \langle \mathcal{V}, \mathcal{E}, \psi \rangle$  is a DDI networks such that:

$$\psi : \mathcal{V} \rightarrow \mathbb{R}^k$$

$$\psi(v) = \langle \psi_v^1, \dots, \psi_v^k \rangle$$

where  $\psi_v^i$  represents the  $i$ -th chemical characteristic of drug  $v$ . The chemical matching coefficient between two drugs  $u$  and  $v$  is defined as follows:

$$CMC(u, v) = \frac{1}{n} \sum_{n=1}^k \sigma_n(u, v), \quad (2)$$

where  $\sigma_n(u, v)$  is equal to 1 if  $|\psi_u^n - \psi_v^n| < \epsilon_n$  and it is equal to 0 otherwise. To find the appropriate threshold, we proceed as follows: Suppose

$$Y^n = \{|\psi_u^n - \psi_v^n| \text{ for all } u, v \in \mathcal{V}\}$$

be a distribution of scalar difference of nodes in  $m$  feature. The cumulative distribution of this feature is defined as follows:

$$F_{Y^n}(y) = \{y_i \in Y^n \mid y_i \leq y\}$$

Now we calculate the quantile values of each distribution as follows:

$$Q_{Y^n}(\tau) = \inf\{y \in Y^n \mid F_{Y^n}(y) \geq \tau\}$$

In this study,  $\epsilon_n = Q_{Y^n}(0.1)$  is considered. In other words, a part of the nodes corresponding to each feature is assumed to be similar when we assume that 0.1 communities are similar to each other.

**Knowledge graph:** To define the weighted graph  $\mathcal{G} = \langle \mathcal{V}, \mathcal{E}, \mathcal{W} \rangle$  of a DDI network, we use the combination of 2 similarity of chemical matching coefficient and Jaccard similarity between two drugs. The weight of each edge in the DDI network is calculated as follows:

$$W(u, v) = \alpha * J_{sim}(u, v) + (1 - \alpha) * CMC(u, v) \quad (3)$$

The scalar nature of this measure provides a quantitative assessment of the similarity between two drugs. In other words, the accuracy of the edge weight plays a crucial role in detecting drug similarity, particularly concerning graph topological similarity (Jaccard) and chemical structure similarity (chemical matching coefficient). These two types of similarity, topological and chemical, address distinct facets of drug similarity. The primary challenge lies in effectively combining these forms of similarity to enhance results when the similarity between two drugs aligns with their similarity weight. In equation (3), the hyperparameter  $\alpha \in [0, 1]$  is employed to strike a balance between structural and chemical similarity.

### 2.3 NGMG method

Each of the chemical features on their own provides quantitative insights into the relationships between drugs. We aim to introduce an algorithm that enhances the DDI network by combining these chemical features with the network’s inherent topological characteristics. To achieve this, we initially partition the network into  $k$  clusters, each illustrating the connections among the drugs within that specific cluster. Suppose  $\mathcal{G} = \langle \mathcal{V}, \mathcal{E}, \mathcal{W} \rangle$  is a weighted network, also suppose  $w^i = \langle w_{i1}, \dots, w_{in} \rangle$  is a vector in  $\mathbb{R}^n$  space such that:

$$w_{ij} = \begin{cases} \mathcal{W}(i, j) & \text{if } e_{ij} \in E \\ 0 & \text{otherwise} \end{cases} \quad (4)$$

Now we define an affinity matrix  $A = [a_{ij}]_{(n \times n)}$  as follows:

$$a_{ij} = \begin{cases} e^{-\frac{-1w^i - w^j}{2\sigma}} & \text{if } e_{ij} \in E \\ 0 & \text{otherwise} \end{cases} \quad (5)$$

Suppose  $L = D^{-\frac{1}{2}}AD^{\frac{1}{2}}$  is an  $n \times n$  matrix so that  $D = [d_i]_{(n \times n)}$  is a diagonal matrix where  $d_i = \sum_{j=1}^n a_{ij}$ . Now suppose that  $\lambda_1, \dots, \lambda_k$ , are the  $k$  largest eigenvalue of matrix  $L$ , and  $x_1, \dots, x_k$ , are the  $k$  eigenvectors corresponding to the eigenvalues ( $k$  is the number of desired clusters). In this case, we define the  $n \times k$  matrix corresponding to this  $k$  eigenvector as  $X = [x_1, \dots, x_k]_{(n \times k)}$  so that the  $j$ -th column of this matrix corresponds to the eigenvalue  $x_j$  with  $n$  elements. The normalized matrix of the  $X$  matrix is called  $Y$  and each row of the matrix  $Y_{(n \times k)} = \begin{pmatrix} y^1 \\ \vdots \\ y^n \end{pmatrix}$  can be considered as a point in  $\mathbb{R}^k$  and we cluster  $n$  points  $y^1, \dots, y^n$  into  $k$  clusters  $C = \{C_1, \dots, C_k\}$  by k-means algorithm. Finally, if the point  $y^i$  is assigned to the cluster  $C_j$ , we assign the  $i$ -th node to the cluster  $C_j$ .

### 2.4 Feature extraction

We extracted the drugs’ chemical structure information using SMILES strings from the XML file provided by DrugBank and extracted chemical features from their SMILES as follows:

- **Chirality:** A chiral center, often found in carbon atoms with four distinct atom groups arranged tetrahedrally, is a type of stereo center. Chiral molecules possess non-superimposable mirror images. Enantiomers, known as R (right-handed) or S (left-handed), are two stereo-isomers of a chiral molecule. When chiral centers are larger, they contribute to the molecule’s increased three-dimensionality, resulting in a reduction of off-target effects and drug-drug interactions [27].

- **Number of C=C and C=N bonds:** The count of carbon-carbon and carbon-nitrogen double bonds indicates the degree of saturation within the molecule. Saturation pertains to the quantity of single bonds present in the molecule. Elevating the number of carbon-carbon and carbon-nitrogen double bonds would, in turn, raise the likelihood of experiencing off-target effects [27].
- **Number of sp<sup>3</sup> :** It denotes the count of carbon atoms with four single bonds, a descriptor quantifying the degree of saturation within the molecule. A higher presence of sp<sup>3</sup> carbon atoms indicates increased saturation, which, in turn, correlates with a reduced likelihood of drug-drug interactions and off-target effects [28].
- **LogS:** Solubility in the context of a drug refers to the maximum quantity of that drug that can dissolve in a given volume of water, typically measured in mol/L. The drug’s solubility is positively associated with its potency, as drugs with higher solubility tend to exhibit fewer drug-drug interaction effects [28].

A higher count of chiral centers, a reduced number of double carbon-carbon and carbon-nitrogen bonds, and an elevated presence of sp<sup>3</sup> carbon atoms within a molecule contribute to more favorable ligand positioning within a protein’s active site. This results in stronger ligand-protein interactions, ultimately leading to a reduction in off-target effects and drug-drug interactions. In summary, multiple stereo groups, aliphatic rings, and single bonds enhance the molecule’s three-dimensionality, amplifying ligand-protein interactions and decreasing drug-drug interactions. Additionally, an increase in the molecule’s sp<sup>3</sup> character, signifying a more significant proportion of spatial carbon atoms with single bonds, correlates with ligand solubility. We extracted and used these informative features to build our knowledge graph.

### 3 Experimental results

In this section, we begin by presenting the NGMG hyperparameters. Subsequently, we perform a comparative analysis of NGMG against other established methods in DDI prediction. Finally, we conduct a case study to explore the specific drug pairs that contribute to potential DDIs. All the materials and implementations are available at: [https://github.com/MahnazHabibi/DDI\\_cluster](https://github.com/MahnazHabibi/DDI_cluster).

#### 3.1 DDI network properties

Here, we present a summary of key statistics related to the DDI network  $G$ . The network exhibits an average node degree of 147.08. Figure 1 illustrates the frequency distribution of DDI network degrees across specific intervals. Our analysis reveals that over 1320 nodes in the network exhibit degrees ranging between 1 and 67. Nodes within the degree range of 67 to 133 are the most prevalent among all nodes. Of the 4375 nodes, 1747 fall within the 67-133 interaction degree range, accounting for 40 % of all drug interactions within this network.

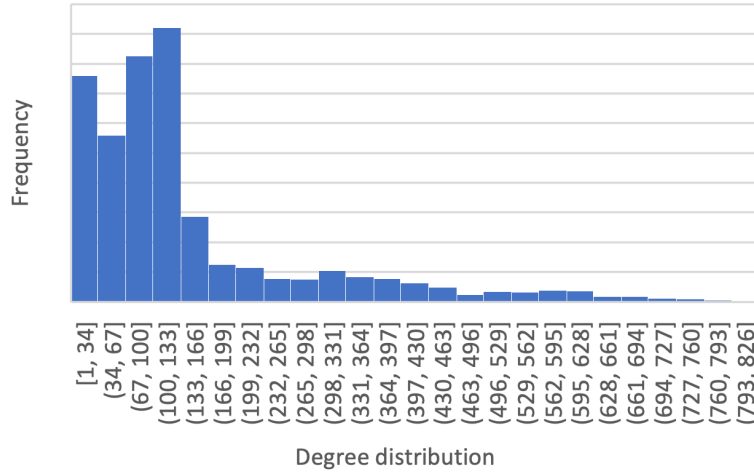


**Fig. 1.** The frequency distribution of DDI network degrees across specific intervals.

The highest degree of node is related to the drug "Thalidomide", which interacts with 1062 other drugs, and the lowest level of interaction is related to the drug "L-Glutamine", which has only one reported interaction with 'Lactulose'.

### 3.2 Parameter Setting

One of the evaluation methods for determining the optimal number of clusters in clustering algorithms is the Silhouette score. This score relies on distance measures between objects within clusters. However, in our network, we deal with drug similarity rather than distance. To address this, we have defined a score for assessing our clustering method, which is analogous to the Silhouette evaluation score.

Let  $C = \{c_1, c_2, \dots, c_k\}$  represent a cluster within our drug dataset, and  $S = [s_{ij}]$  denote the similarity matrix between drugs, with  $s_{ij} = w(i, j)$  for each drug  $i$  and  $j$ . For each drug  $i \in c_i$  in cluster  $C_i$ , we define the average similarity of this drug with other drugs as follows:

$$A(i) = \frac{1}{(|c_i| - 1)} \sum_{k \in c_i} s_{ik} \quad (6)$$

Similarly, the most similarity of this node with other clusters is defined as follows.

$$B(i) = \max\left\{\frac{1}{(|c_j|)} \sum_{k \in c_j} s_{ik} ; c_j \neq c_i\right\} \quad (7)$$

Finally, the score of each drug  $i$  corresponding to clustering  $C$  is defined as follows:

$$s(i) = \frac{A(i) - B(i)}{\max(A(i), B(i))} \quad (8)$$

The value of this score is between -1 and 1 for each drug, and the closeness of this number to 1 indicates that this drug is more similar to the drugs that are placed together in one cluster than to drugs in other clusters.

The average score of all drugs in each cluster  $c_i$  is shown with the symbol  $s(c_i)$  and is defined as follows:

$$s(c_i) = \frac{1}{|c_i|} \sum_{j \in c_i} s_j \quad (9)$$

Now, we define the score for a clustering  $C$  as a the percentage of clusters whose value of  $s(c_i)$  in them is greater than 0 in other words:

$$Score(C) = \frac{|\{c_i \in C ; s(c_i) > 0\}|}{|C|} \quad (10)$$

Finally, The clustering algorithm was executed for values of  $k$  ranging from 1 to 100. We identified the optimal number of clusters as  $k = 44$ , where the clustering score,  $Score(C)$ , exceeded 0.8, specifically reaching 0.83. This means that over 83% of the clusters within this clustering have an average score greater than zero.

### 3.3 Evaluation of NGMG based on random sets

To assess the NGMG algorithm, we utilize two distinct methodologies. Initially, we apply our algorithm to a network containing 20% false positives and 20% false negatives. Due to the prevalence of false positives and negatives in biological data, we evaluate our algorithm's sensitivity by randomly introducing and eliminating 20% of edges. This process results in clusters  $C = c_1, \dots, c_k$  derived from the knowledge graph. Additionally, by introducing (or removing) 20% randomness in the edges of the DDI network, a new knowledge graph is formed. Subsequently, clusters  $S = s_1, \dots, s_k$  are derived from this altered, random knowledge graph. To compare clusters obtained from each of these modified graphs, we employ a metric based on the proportion of nodes within a cluster that coincide with clusters from the original DDI network. If  $S$  represents a cluster from the random network and  $C$  denotes a cluster from the original network, with sizes  $|S|$  and  $|C|$ , the matching score for this cluster is defined as follows:

$$J_{sim}(u, v) = \frac{|S \cap C|^2}{|S||C|} \quad (11)$$

If the intersection of  $S$  and  $C$  meets or exceeds the threshold  $\theta$ , we consider the two clusters to be matched. In this study, we have adjusted the thresholds



from 0.2 to 0.8. In Table 1, we iterated the process of adding or removing 20% of the edges 10 times and presented an average of the percentage of matched clusters for each of the random graph with the initial knowledge graph. The subsequent table illustrates that, on average, when removing 20% of the edges from the primary graph, 50% of the resulting clusters exhibit an overlap greater than 0.5 ( $\theta > 0.5$ ) with the primary graph clusters. Similarly, by introducing 20% of the edges to the primary graph, on average, 50% of the derived clusters have an overlap of more than 0.7 ( $\theta > 0.7$ ) with the primary graph clusters. This observation indicates that our algorithm is robust and it can refine false positives and false negatives with the help of chemical properties.

**Table 1.** The percentage of clusters with an overlap of more than  $\theta$  with the clusters of the original knowledge graph.

Threshold( $\theta$ )	Add	Remove
0.2	0.84	0.77
0.3	0.79	0.75
0.4	0.68	0.63
0.5	0.61	0.5
0.6	0.56	0.40
0.7	0.5	0.38
0.8	0.35	0.31

### 3.4 Evaluation of NGMG clusters

To enhance the assessment of the NGMG algorithm’s outcomes, we evaluate the clusters obtained by our algorithm based on the interactions collected by the BioSNAP group as a new DDI network [29]. This collection comprises 48514 interactions among 1514 drugs approved by the U.S. Food and Drug Administration. Among the 1514 drugs in this network, 1008 drugs are encompassed in the DDI network under our investigation, denoted as the set of drugs  $V$ . Out of the 44 obtained drug clusters, 35 clusters include at least one drug from the total of 1008 common drugs present in both datasets. Subsequently, if  $E$  represents a set of presumed interactions within the set of drugs  $V$ , the count of edges with both ends in the one of the resulted clusters of our methods is termed the sum of internal edges, called as *In\_Edges*. Set  $E_1$  is a set of edges of the primary DDI network, the ends of which are in the set  $V$  and set  $E_2$  shows the set of edges of the second DDI network (BioSANP), the two ends of which are in the set  $V$ . Table 2 displays the count of internal cluster edges for each of the mentioned sets.

As observed in the Table 2, the clusters generated by our algorithm retain a significant portion of intra-cluster connections among the drugs within each cluster, even when exposed to a new DDI network. Despite the distinct topological characteristics, the overlap of edges within a cluster for the primary DDI

**Table 2.** Comparison between edge placement in our clusters for the initial DDI and SNAP DDI.

Set	No. Edges	No. In_Edges	No. Out_Edges
$E_1$	58393	39124 (%67)	19270 (%33)
$E_2$	25881	16305 (%63)	9576 (%37)
$E_1 \cap E_2$	11337	8274 (%73)	3063 (%27)
$E_1 \cup E_2$	72937	43032 (%59)	29905 (%41)

network and the secondary DDI network remains notably high. As depicted in the table, 73% of the edges within the primary DDI network’s clusters persist as shared within these two sets.

## 4 Conclusions

We introduced a novel method called NGMG to forecast potential Drug-Drug Interactions. NGMG constructs a knowledge graph, learning the chemical and topological features of each drug from its SMILE and interaction properties. The acquired features of each drug pair were concatenated to create the final DDI prediction score. Our experimental findings indicate that NGMG outperformed in both scenarios: predicting potential DDIs among known drugs and between known drugs and new drugs. Additionally, the performance of drug features directly learned by NGMG, derived from chemical properties, effectively identified false positive and false negative interactions among drugs in different scenarios. This study aimed to identify informative clusters of drugs with similar chemical and topological properties, rather than predicting direct connections between drugs. In our forthcoming research, we aim to utilize the insights gained from this study and we plan to incorporate other similarity measures to predict edges between drugs, refining our DDI network’s accuracy in understanding drug interactions.

## References

1. Cheng F, Kovács I.A, Barabási A.L : Network-based prediction of drug combinations. *Nat. Commun* **10**1197 (2019).
2. Zhu A.X, Finn R.S, Edeline J, Cattan S, Ogasawara S, et al. :Pembrolizumab in patients with advanced hepatocellular carcinoma previously treated with sorafenib (KEYNOTE-224): A non-randomised, open-label phase 2 trial. *Lancet Oncol* **19** 940–952 (2018).
3. Entacapone/levodopa/carbidopa combination tablet: Stalevo. *Drugs R&D* **4** 310–311 (2003).
4. Niu J, Straubinger R.M, Mager D.E :Pharmacodynamic Drug-Drug Interactions. *Clin. Pharmacol. Ther* **105** 1395–1406 (2019).
5. Aghdam R, Habibi M, Taheri G. Using informative features in machine learning based method for COVID-19 drug repurposing. *Journal of chem* **131**-4 (2021).

6. Habibi M, Taheri G, Aghdam R. A SARS-CoV-2 (COVID-19) biological network to find targets for drug repurposing. *Scie Rep* **11** 9378 (2021).
7. Zhang W, Chen Y, Liu F, Luo F, Tian G, Li X: Predicting potential drug-drug interactions by integrating chemical, biological, phenotypic and network data. *BMC Bioinform* **18** 18 (2017).
8. Kastrin A, Ferk P, Leskošek B: Predicting potential drug-drug interactions on topological and semantic similarity features using statistical learning. *PLoS ONE* **13** e0196865 (2018).
9. Yu H, Mao K.T, Shi J.Y, Huang H, et al. : Predicting and understanding comprehensive drug-drug interactions via semi-nonnegative matrix factorization. *BMC Syst. Biol* **12** 101–110 (2018).
10. Zhang S. SFLLN: A sparse feature learning ensemble method with linear neighborhood regularization for predicting drug–drug interactions. *Inf. Sci* **497** 189–201 (2019).
11. Sridhar D, Fakhraei S, Getoor L : A probabilistic approach for collective similarity-based drug–drug interaction prediction. *Bioinform* **32** 3175–3182 (2016).
12. Gottlieb A, Stein G.Y, Oron Y, Ruppin E, Sharan R, INDI: A computational framework for inferring drug interactions and their associated recommendations. *Mol. Syst. Biol* **8** 592 (2012).
13. Cheng F, Zhao Z: Machine learning-based prediction of drug–drug interactions by integrating drug phenotypic, therapeutic, chemical, and genomic properties. *J. Am. Med Inform. Assoc.* **21** e278–e286 (2014).
14. Feng Y.H, Zhang S, Shi J. DPDDI: A deep predictor for drug-drug interactions. *BMC Bioinform* **21** 419 (2020).
15. Zhang P, Wang F, Hu J, Sorrentino R : Label Propagation Prediction of Drug-Drug Interactions Based on Clinical Side Effects. *Sci. Rep* **5** 12339 (2015).
16. Habibi M, Taheri G.: Topological network based drug repurposing for coronavirus 2019. *Plos one.* **16**(7), e0255270. (2021)
17. Wu Z, Pan S, Chen F, Long G, Zhang C, Philip SY : A comprehensive survey on graph neural networks. *IEEE trans on NN and learning systems* **32** 4-24 (2020).
18. Taheri G, Habibi M. Identification of essential genes associated with SARS-CoV-2 infection as potential drug target candidates with machine learning algorithms. *Scie Rep* **13**15141 (2023).
19. Han L, Sayyid Z.N, Altman R.B : Modeling drug response using network-based personalized treatment prediction (NetPTP) with applications to inflammatory bowel disease. *PLoS Comput. Biol* **17** e1008631 (2021).
20. Yang J, Li A, Li Y, Guo X, Wang M : A novel approach for drug response prediction in cancer cell lines via network representation learning. *Bioinfo* **35** 27–1535 (2018).
21. Le D.H, Pham V.H, Drug Response Prediction by Globally Capturing Drug and Cell Line Information in a Heterogeneous Network. *J. Mol. Biol* **430** 2993–3004 (2018).
22. Wang F, Lei X, Liao B, Wu F.X: Predicting drug–drug interactions by graph convolutional network with multi-kernel. *Brief. Bioinform* **23** (2021).
23. Liu S, Huang Z, Qiu Y, Chen YP, Zhang W. Structural network embedding using multi-modal deep auto-encoders for predicting drug-drug interactions. In2019 IEEE Inte conf BIBM. 445-450 (2019)
24. Jia P, Hu R, Pei G, Dai Y, et. al. : Deep generative neural network for accurate drug response imputation. *Nat. Commun* **12** 1740 (2021).
25. Gerdes H, Casado P, Dokal A, et al. Drug ranking using machine learning systematically predicts the efficacy of anti-cancer drugs. *Nat. Commun.* **12** 1850 (2021).

26. Wishart D.S, Feunang Y.D, Guo A.C, Lo E.J, et al. DrugBank 5.0: A Major Update to the DrugBank Database for 2018. *Nucleic Acids Res.* **46** D1074–D1082 (2018).
27. Chandrasekaran B, Abed SN, Al-Attraqchi O, Kuche K, Tekade RK. Computer-aided prediction of pharmacokinetic (ADMET) properties. In *Dosage form design* para 731-755(2018).
28. Bohnert T, Prakash C. ADME profiling in drug discovery and development: an overview. *Encyclopedia of drug metabolism and interactions.* **16** 1-42 (2011).
29. Zitnik M, Sosis R, Leskovec J. BioSNAP Datasets: Stanford biomedical network dataset collection. Note: <http://snap.stanford.edu/biodata>. **5** (2018).